

Time Scale Analysis of Receptor Enzyme Activity

Irreversible Inhibition Sometimes Exhibits Incubation-time Independence

Tao You

Computational Biology, Discovery Sciences
Innovative Medicines & Early Development
AstraZeneca, Alderley Park, Cheshire, SK10 4TG, UK
youtao80@gmail.com

Hong Yue

Department of Electrical and Electronic Engineering
University of Strathclyde, Glasgow, G1 1XW, UK
hong.yue@strath.ac.uk

Abstract—At early drug discovery, purified protein-based assays are often used to characterise compound potency. As far as dose response is concerned, it is often thought that a time-independent inhibitor is reversible and a time-dependent inhibitor is irreversible. Using a simple kinetics model, we investigate the legitimacy of this. Our model-based analytical analysis and numerical studies reveal that dose response of an irreversible inhibitor may appear time-independent under certain parametric conditions. Hence, time-independence cannot be used as evidence for inhibitor reversibility. Furthermore, we also analysed how the synthesis and degradation of a target receptor affect drug inhibition in an *in vitro* cell-based assay setting. Indeed, these processes may also influence dose response of an irreversible inhibitor in such a way that it appears time-independent under certain conditions. Hence, time-independent dose response in a cell assay also needs careful considerations. It is necessary to formulate a suitable model for analysis of protein-based assay and *in vitro* cell assay data to ensure a consistent understanding.

Keywords—irreversible inhibition; model of receptor turnover; fast drug process; slow drug process; time-scale analysis

I. INTRODUCTION

Drug discovery and development typically involve protein-based assay, *in vitro* cell assay, *in vivo* animal assay and clinical trials. These studies are often organised in this particular temporal order, in the hope that the results of a previous step (e.g. protein-based assay) will help inform the design and interpretation of the subsequent experiment (e.g. *in vitro* cell assay).

A new paradigm that helps enable robust translation of each type of study arises in recent years [1]. Known as Systems Pharmacology, it employs multi-scale modelling approaches to integrate heterogeneous types of data generated under diverse experimental conditions spanning different temporal and dimensional scales [2]. These models are able to reconcile different experimental conditions, such as *in vitro* cell assays and *in vivo* animal models [3], and to bridge preclinical models with clinical trials with an endeavour to generate statistically robust predictions that are validated with preclinical and clinical data [4].

While multi-scale modelling has been successfully deployed in drug development programmes, its application in

early drug discovery has been more limited [5]. In fact, there is an urgent need to develop Systems Pharmacology so as to better bridge protein-based assay and *in vitro* cell assay [1].

Cellular kinetics may sometimes not be fully appreciated by medicinal chemists who design protein-based assays, and this limits its application. For instance, the potency of a chemical entity to inhibit an enzyme is often characterised by IC_{50} , the chemical concentration that generates half of maximal inhibition. For an irreversible inhibitor that covalently modifies a purified target enzyme *in vitro*, the chemical reaction tends more complete given a longer drug incubation period. Consequently, IC_{50} usually exhibits incubation time-dependent shift, making the inhibitor appear more potent at long incubation periods [6, 7].

In contrast, a target protein in a living cell undergoes synthesis and degradation, which are often regulated via gene regulations and cell signalling. These processes typically happen within minutes and hours [8]. This may influence cellular response to drug inhibition. In other words, shooting a moving target in a cell might be different from shooting an immobile target in a protein-based assay. In this study, we investigate how cellular response is influenced by both drug parameters and cell parameters.

II. A MODEL OF RECEPTOR TURNOVER AND IRREVERSIBLE INHIBITION

A simple model is proposed to recapitulate receptor turnover (i.e. synthesis and degradation) and drug inhibition.



In process (1), receptor R is synthesized at a constant rate k_p , and degrades following a first-order kinetics with a rate constant k_d . For the sake of simplicity, this model does not consider feedback mechanism that regulates either synthesis or degradation. In process (2), a drug molecule first binds R reversibly to comprise an intermediate complex C with apparent association and dissociation rates k_{on} and k_{off} , respectively. The complex C then forms a covalent bound

irreversibly at the second step, in a first-order reaction with a rate constant k_i . Based on mass-balance principle, the corresponding ordinary differential equations (ODEs) for concentrations of R and C are

$$\frac{dR}{dt} = -(k_d + k_{on})R + k_p + k_{off}C \quad (3)$$

$$\frac{dC}{dt} = k_{on}R - (k_{off} + k_i)C \quad (4)$$

with the following units: nM for R , C ; nM/min for k_p ; and 1/min for k_d , k_{on} , k_{off} and k_i .

In the absence of drug, the receptor has a steady state at $R_0 = k_p/k_d$ nM. Scaling R and C with R_0 , they become dimensionless $r = R/R_0 = Rk_d/k_p$, $c = C/R_0 = Ck_d/k_p$. ODEs (3) and (4) are written as

$$\frac{dr}{dt} = -(k_d + k_{on})r + k_d + k_{off}c \quad (5)$$

$$\frac{dc}{dt} = k_{on}r - (k_{off} + k_i)c \quad (6)$$

This model takes a dimensionless form, when k_{off} is used to scale the time term by $\tau = k_{off}t$, and to scale reaction rates by $\kappa_{on} = k_{on}/k_{off}$, $\kappa_i = k_i/k_{off}$, and $\kappa_d = k_d/k_{off}$.

$$\frac{dr}{d\tau} = -(\kappa_{on} + \kappa_d)r + c + \kappa_d \quad (7)$$

$$\frac{dc}{d\tau} = \kappa_{on}r - (1 + \kappa_i)c \quad (8)$$

Note all terms in (7) and (8) are dimensionless, including concentration variables r and c , time τ , and parameters κ_{on} , κ_i , κ_d . The synthesis rate k_p is included in κ_d through scaling $\kappa_d = k_d/k_{off} = k_p/(k_{off}R_0)$. The initial conditions of this model are set to be $r_0 = r(0) = 1$ and $c_0 = c(0) = 0$.

With this dimensionless model, the analysis of system behaviour under different parametric regimes can be discussed in a consistent scheme.

III. FAST DRUG PROCESS RELATIVE TO RECEPTOR TURNOVER

The parametric regimes have been divided into that of fast drug process and slow drug process. We first discuss the conditions of fast drug binding and dissociation.

A. Fast Drug Binding and Dissociation Relative to Receptor Turnover

The parametric regime is defined by $k_{off} \gg k_d$, and $k_{on} \gg k_d$. In this case, the receptor turnover rate k_d is much smaller than the drug binding and dissociation rates k_{on} and k_{off} .

- When $k_{off} \gg k_d$, i.e., $\kappa_d \ll 1$, the period of target coverage (characterized by $1/k_{off}$) is much shorter than that of

receptor degradation (characterized by $1/k_d$), which can be due to: i) short target coverage, i.e., $k_{off} \gg 1$; ii) slow receptor degradation, i.e., $k_d \ll 1$; and iii) combination of i) and ii).

- When $k_{on} \gg k_d$, i.e., $\kappa_{on} \gg \kappa_d$, a receptor binds a drug molecule at a rate much faster than its degradation.

Under these conditions, the term of κ_d can be ignored, and the model is approximated by

$$\begin{aligned} \frac{dr}{d\tau} &= -\kappa_{on}r + c \\ \frac{dc}{d\tau} &= \kappa_{on}r - (1 + \kappa_i)c \end{aligned} \quad (9)$$

How small does k_d have to be in comparison to k_{off} and k_{on} to ensure the validity of this approximation? This is examined by the following numerical simulation. Firstly, the full model in (7) and (8) are simulated with $\kappa_{on} = 1$ ($k_{on} = k_{off}$) and $\kappa_i = 0.001$ ($k_{off} \gg k_i$), when $\kappa_d = 10^{-6}$ (Fig. 1(a)), and $\kappa_d = 10^{-4}$ (Fig. 1(b)), respectively. The approximated model in (9) is simulated using identical values for κ_{on} and κ_i , as shown in Fig. 1(c). All simulations are performed for four different incubation time periods, including 10^{-3} , 1, 10^3 and 10^6 . It can be observed that the responses in Fig. 1(a) are close to those in Fig. 1(c), which suggests that when $\kappa_d \leq 10^{-6}$, model (9) provides a good approximation to the full model in (7) and (8).

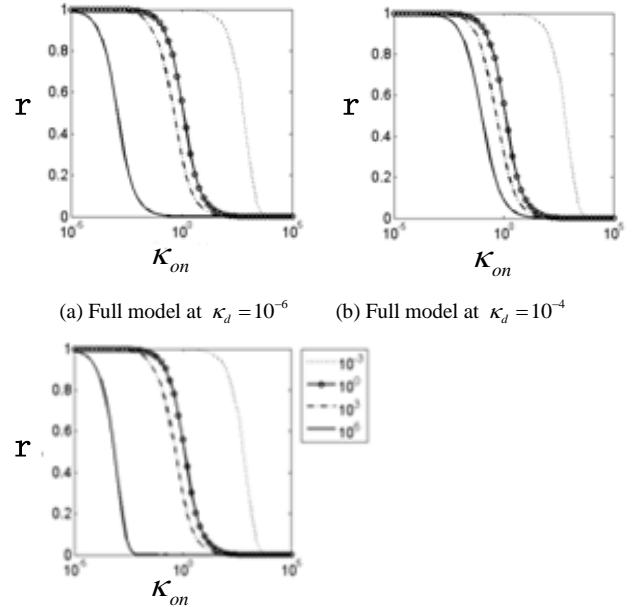


Fig. 1. Dose response curves predicted for different incubation time, when $k_{on} = 1$ and $k_i = 0.001$. Incubation times shown in the figure legend (10^{-3} , 10^0 , 10^3 , 10^6) are in τ . (a) Full model (7) and (8) simulated at $\kappa_d = 10^{-6}$; (b) Full model simulated at $\kappa_d = 10^{-4}$; (c) Simulation from the approximate model in (9). In all figures, k_{on} is plotted in \log_{10} scale.

Denoting $X = [r \ c]^T$, the simplified model in (9) can be written as a homogeneous system model,

$$\dot{X} = AX, \quad \text{where } A = \begin{bmatrix} -\kappa_{on} & 1 \\ \kappa_{on} & -(1+\kappa_i) \end{bmatrix} \quad (10)$$

We can use the eigenvalue method to analyse this system. Denoting the trace and determinant of matrix A as $T = \text{trace}(A) = -(1+\kappa_{on} + \kappa_i)$, $\Delta = \det(A) = \kappa_{on} \cdot \kappa_i$, the eigenvalues of A are calculated by $\lambda_{1,2} = \left(T \pm \sqrt{T^2 - 4\Delta}\right)/2$.

For $\lambda_1 = \frac{T + \sqrt{T^2 - 4\Delta}}{2}$, the associated eigenvector is

$$v_1 = [v_{11} \ v_{12}]^T = \left[\frac{1+\kappa_i - \kappa_{on} + \sqrt{(1+\kappa_{on} + \kappa_i)^2 - 4\kappa_{on}\kappa_i}}{2\kappa_{on}} \ 1 \right]^T.$$

For $\lambda_2 = \frac{T - \sqrt{T^2 - 4\Delta}}{2}$, the associated eigenvector is

$$v_2 = [v_{21} \ v_{22}]^T = \left[\frac{1+\kappa_i - \kappa_{on} - \sqrt{(1+\kappa_{on} + \kappa_i)^2 - 4\kappa_{on}\kappa_i}}{2\kappa_{on}} \ 1 \right]^T.$$

With initial conditions $r_0 = 1$ and $c_0 = 0$, the analytical solutions for (10) are

$$r(t) = \frac{1}{v_{11} - v_{21}} (v_{11} e^{\lambda_1 t} - v_{21} e^{\lambda_2 t})$$

$$c(t) = \frac{1}{v_{11} - v_{21}} (e^{\lambda_1 t} - e^{\lambda_2 t})$$

The \log_{10} transformed ratio of the two eigenvalues for different pairs of κ_{on} and κ_i is plotted in a heat map (Fig. 2). This diagram shows that when both parameters have similar values and are above 1, λ_1 and λ_2 are close to each other (the red area in Fig. 2). In this case, the system has only one time scale in this parametric regime. However, if either parameter is much larger than 1 or both parameters are much smaller than 1, then $|\lambda_1|/|\lambda_2| \ll 1$ (the blue area in Fig. 2), and two different time scales exist, including a slow time scale characterized by $1/|\lambda_1|$ and a fast time scale characterized by $1/|\lambda_2|$ (note T is negative).

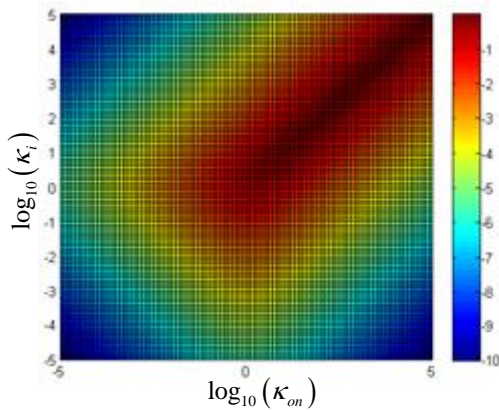


Fig. 2. $\log_{10}(\lambda_1/\lambda_2)$ plotted as a function of $\log_{10}(\kappa_{on})$ and $\log_{10}(\kappa_i)$. Values between -10 and 0 are colour-coded.

In the following, we will study several special cases within this parametric regime.

B. Fast Drug Dissociation Relative to Covalent Modification

Under the condition of fast drug process over receptor turnover ($k_{off} \gg k_d$, and $k_{on} \gg k_d$), we further consider the regime of $k_{off} \gg k_i$, i.e., $\kappa_i \ll 1$. This means the drug dissociation is much faster than the covalent modification. This corresponds to the lower part of Fig. 2. This condition is satisfied if a) an irreversible inhibitor has to overcome a relatively large energy barrier to covalently modify the receptor, b) drug dissociation is rapid, c) a combination of both. The model can be further simplified as

$$\frac{dr}{d\tau} = -\kappa_{on} r + c$$

$$\frac{dc}{d\tau} = \kappa_{on} r - c \quad (11)$$

In this case, $\frac{dr}{d\tau} = -\frac{dc}{d\tau}$. Hence, $|\Delta|/|T^2| \ll 1$. This means $|\lambda_1| \approx 0$ and $|\lambda_1| \ll |\lambda_2|$. In this case, two different time scales exist, a slow time scale characterized by $1/|\lambda_1|$ and a fast time scale characterized by $1/|\lambda_2|$. The receptor decreases in both time scales.

Denote the scaled incubation times at which two dose response curves are measured by τ_1, τ_2 , respectively. If measurements are taken at incubation times comparable to or much longer than the slow time scale, (i.e. $\tau_{1,2} \sim 1/|\lambda_1|$ or $\tau_{1,2} \gg 1/|\lambda_1|$), then dose responses are mainly determined by changes at the slow time scale. Time-dependency is evident if $\tau_1 \gg \tau_2$ and *vice versa*. This indicates that dose response curves for different incubation times should be separated. On the other hand, for much shorter incubation times, $\tau_{1,2} \ll 1/|\lambda_2|$, dose responses are mainly dependent on changes at the fast, shorter time scale $1/|\lambda_2|$. The two dose response curves are well separated if $\tau_1 \gg \tau_2$, and *vice versa*. In contrast, if $1/|\lambda_2| < \tau_{1,2} < 1/|\lambda_1|$, then dose responses are determined by both time scales. For $1/|\lambda_2| \ll \tau_{1,2} \ll 1/|\lambda_1|$, dose response curves are close to each other following one time scale.

For example, suppose $\kappa_{on} = 1$, $\kappa_i = 0.001$. Then, $T = -2.001$, $\Delta = 0.001$, $\lambda_1 = -5.0 \times 10^{-4}$, $\lambda_2 = -2.0$. $v_1 \approx [1.0 \ 1]^T$, $v_2 \approx [-1.0 \ 1]^T$. Therefore, the time scales are O(3) ($1/|\lambda_1| = 2.0 \times 10^3$) and O(1) ($1/|\lambda_2| \approx 0.50$). The analytical solution to the receptor concentration is approximately $r(\tau) = 0.5(1.0e^{-2.0\tau} + 1.0e^{-0.0005\tau})$ under these parameters.

For $\tau_1 = 0.001, \tau_2 = 1$, dose responses are dominated by the short time scale O(1). In addition, these incubation times are of three orders of magnitude difference. For the same input, dose response curves are expected to be separated (compare the two curves on the left in Fig. 1(c)). Using similar reasoning, dose response curves for $\tau_1 = 1 \times 10^3, \tau_2 = 1 \times$

10^6 are expected to be separated, as both of them are mainly dependent on the fast time scale $O(3)$ (the two curves on the right in Fig. 1(c)). For $\tau_1 = 1, \tau_2 = 1000$, dose response curve taken at $1 \times k_{off}$ is mainly determined by the fast time scale $e^{-2 \times 1}$, while the one taken at $1000 \times k_{off}$ is mainly determined by the slow time scale $e^{-0.0005 \times 1000}$. Therefore, both dose response curves are close to each other (the two curves in the middle of Fig. 1(a)).

In summary, for an irreversible inhibitor that dissociates quickly or has to overcome a large energy barrier to covalently modify a receptor, if the receptor undergoes very slow synthesis and degradation, two time scales exist for dose response. Dose response curves measured at different incubation times can be either close to each or widely separated, depending on the incubation time relative to the two time scales. Therefore, incubation time-independence in dose response does not necessarily suggest drug inhibition is reversible.

In practice, if $k_i \ll k_{off}$ is known beforehand, the drug should be incubated for a period of time that is comparable to $1/k_i$. Then τ_1 and τ_2 are more likely to be in the long range, say $\tau_{1,2} \gg 10^3 \times k_{off}$. This leads to time-dependent dose responses and avoids confusion of taking the drug as a reversible inhibitor.

C. Fast Drug Binding/Dissociation and Fast Covalent Modification Relative to Receptor Turnover

The parametric regime is classified by: $k_{on} \gg k_d, k_{off} \gg k_d, k_i \gg k_d$, and $k_i \approx k_{on}$. In this case, both reversible binding/dissociation and irreversible modification are faster than receptor turnover. The approximate model is the same as (9). According to Fig. 2, λ_1 and λ_2 are close to each other. Hence, the system has only one time scale that is approximately $O(|\lambda_1|^{-1})$ (and equally $O(|\lambda_2|^{-1})$). Therefore, dose response curves measured at different incubation times are predicted to be separated from each other (Fig. 3).

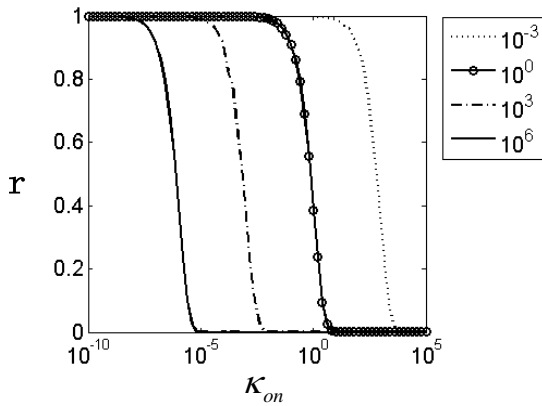


Fig. 3. Dose response curves predicted for different incubation times. Incubation times shown in the figure legend ($10^{-3}, 10^0, 10^3, 10^6$) are in τ , $k_i = k_d = 10$.

IV. SLOW DRUG PROCESS RELATIVE TO RECEPTOR TURNOVER

A. Slow Drug Dissociation Relative to Receptor Turnover

The parametric regime is defined by $k_{off} \ll k_d$, i.e., $k_d \gg 1$. The target coverage rate is much slower than the receptor degradation rate, which can be due to: i) long period of target coverage; ii) fast receptor degradation; and iii) combination of both. This might be biologically relevant when receptor homeostasis is tightly regulated at the turnover level. The full model in (7) and (8) is used for this condition.

This is an inhomogeneous system, which cannot be simply analysed by eigenvalue methods. To avoid using tedious mathematical formulation in the discussion, numerical studies are performed to analyse the dose response behaviour.

Similar to Fig. 2, we have plotted $\log_{10}(\lambda_1/\lambda_2)$ as a function of κ_{on} and κ_i in \log_{10} scales. For $k_{off} = k_d$, separation of time scales happens if either $k_{on} \gg k_d$ or $k_i \gg k_d$, with the former leads to more pronounced effects (Fig. 4(a)). In contrast, if $k_{off} = 0.001k_d$, separation of time scales can also happen if both $k_{on} \ll k_d$ and $k_i \ll k_d$ (bottom-left area in Fig. 4(b)).

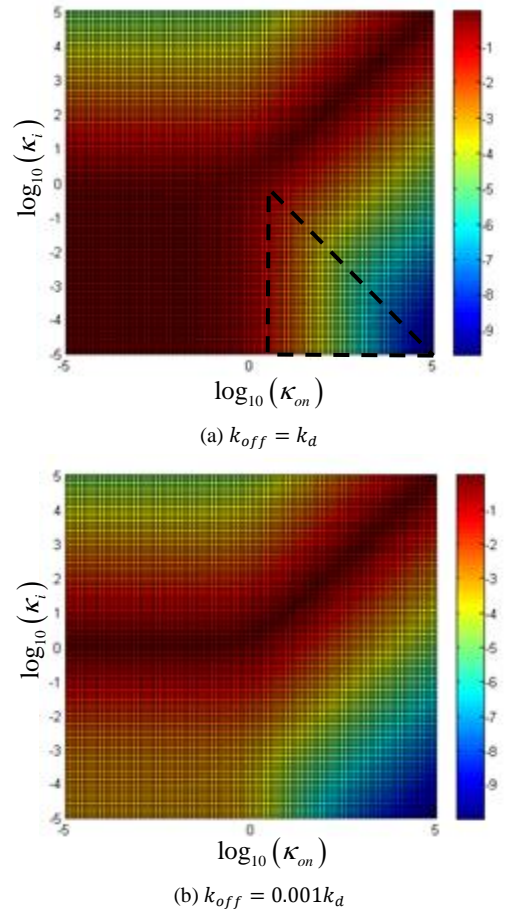


Fig. 4. $\log_{10}(\lambda_1/\lambda_2)$ plotted as a function of κ_{on} and κ_i . (a) $k_{off} = k_d$; (b) $k_{off} = 0.001k_d$. Both axes are in \log_{10} scale. Values between -10 and 0 are colour-coded.

To examine whether separation of time scales dictates time-dependency in dose response, we need to investigate how the factors associated with the exponential functions in receptor's analytical solution compare to each other. Fig. 5 plots $\log_{10}\{|v_{11}\lambda_2(1+\lambda_1)/[v_{21}\lambda_1(1+\lambda_2)]|\}$ as a function of κ_{on} and κ_i in \log_{10} scales. Fig. 5(a) shows when $k_{off} = k_d$, the two factors are comparable for the following regimes:

- i) $k_{on} > k_d, k_i > k_d, k_{on} \approx k_i$;
- ii) $k_{on} < k_d, k_d < k_i < 10k_d$;
- iii) $k_i < k_d, \log_{10}(k_{on}) < -\log_{10}(k_i)$.

Considering both Fig. 4(a) and Fig. 5(a), the only parametric regime that allows separation of time scales and also has comparable factors in front of exponentially decay factors is: $k_{off} = k_d, k_i < k_d, k_{on} > k_d, \log_{10}(k_{on}) < -\log_{10}(k_i)$. This is the region marked by dashed triangles in Fig. 4(a) and 5(a).

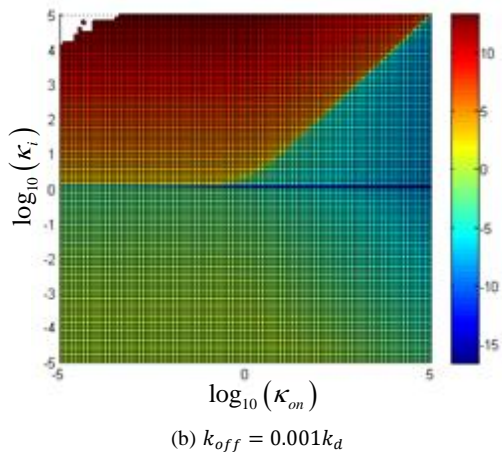
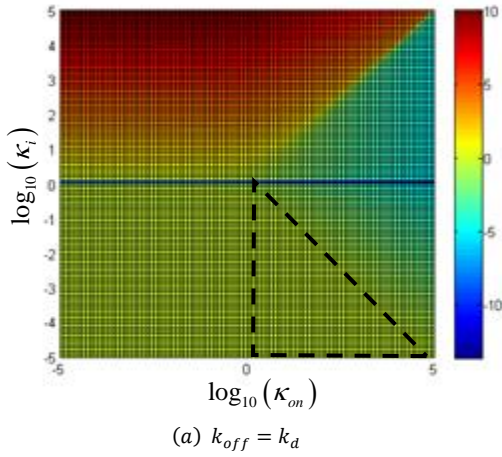


Fig. 5. $\log_{10}\{|v_{11}\lambda_2(1+\lambda_1)/[v_{21}\lambda_1(1+\lambda_2)]|\}$ plotted as a function of κ_{on} and κ_i . (a) $k_{off} = k_d$; (b) $k_{off} = 0.001k_d$. Both axes are in \log_{10} scale. Values between -15 and 10 are colour-coded.

An example is discussed to illustrate these ideas by taking $k_{off} = k_d, k_i \ll k_d$. This means the receptor degradation is as

fast as target coverage and the drug overcomes a large energy barrier to covalently modify the receptor.

Suppose $k_{on} = k_d, k_i = 0.001k_d$. Under this condition, the drug-associated receptor complex continues to rise over time before reaching its equilibrium state. Accordingly, complex dissociation rate keeps increasing until the new equilibrium is reached. Hence, receptor first decreases as a result of drug inhibition, then recovers to a point that is just below the initial condition due to complex dissociation. Apparently, dose response measured before recovery would make the drug appear more potent than the actual steady-state response (compare dotted curve with other curves in Fig. 6). Given the proximity between $|\lambda_1|$ and $|\lambda_2|$, dose response measurement taken at an incubation time that is longer than $1/|\lambda_1|$ are predicted to be close to each other.

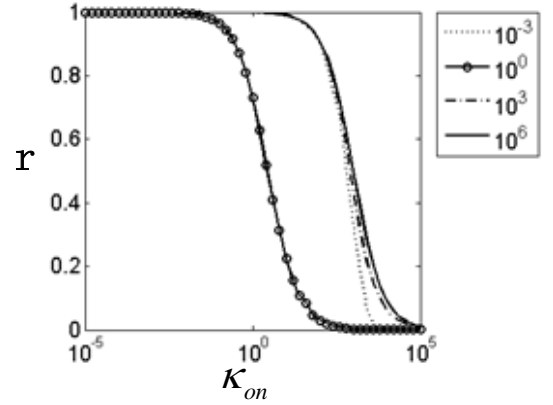


Fig. 6. Dose response curves predicted for different incubation time. (a) Full model is simulated, assuming $k_{off} = k_d, k_i = 0.001k_d$. Incubation times ($10^{-3}, 10^0, 10^3, 10^6$) are in τ .

Alternatively, when $k_{on} = 10000k_d, k_i = 0.001k_d$, then, $T = -10002.001, \Delta = 11.001, \lambda_1 \approx -1.1 \times 10^{-3}, \lambda_2 \approx -1.0 \times 10^4, v_1 \sim [1.0 \times 10^{-4} \ 1]^T, v_2 \sim [-1.0 \times 10^0 \ 1]^T$.

$$r(t) = 9.1 \times 10^{-2} + 1.0 \times 10^0 \times e^{-1.0 \times 10^4 t} - 9.1 \times 10^{-2} e^{-1.1 \times 10^{-3} t}$$

Because $\lambda_1 \ll \lambda_2$, only the fast time scale λ_2 determines dose response. Therefore, dose response is incubation time-dependent.

B. Slow Drug Binding and Fast Covalent Modification Relative to Receptor Turnover

The parametric regime is: $k_{on} \ll k_d \ll k_i$, (upper left corner of Fig. 2). This speaks about an irreversible inhibitor that binds slowly to the receptor but reacts covalently in a fast manner, both relative to receptor degradation. The simplified model is accordingly

$$\begin{aligned} \frac{dr}{d\tau} &= -\kappa_d r + c + \kappa_d \\ \frac{dc}{d\tau} &= \kappa_{on} r - (1 + \kappa_i) c \end{aligned} \quad (12)$$

Similar to the previous case, two different time scales exist for model (12), and the receptor decreases in both time scales.

V. CONCLUSIONS

At lead generation and optimisation, it is important to understand the Mechanism Of Action (MOA) of a chemical compound, as well as the Structure-Activity Relationship (SAR), in the hope that ultimately a compound with sufficient therapeutic efficacy is taken further for preclinical development. Reversibility of a compound is a crucial aspect of MOA characterisation, which is often unknown for compounds coming out of empirical screening methods.

Towards this goal, assays have been established to study inhibition reversibility [9]. It is generally accepted that response to irreversible inhibitors are time-dependent. Hence, it is often taken for granted that time-independence indicates inhibition reversibility. However, our mathematical analysis refutes this. Based on our simulation, for protein-based assays, under certain parameter conditions, the dose response curves can be very similar to each other (compare the middle curves in Fig. 1(C)), given 1000-fold variation in incubation time. In practice, these data might not be statistically different and can be erroneously taken as evidence of reversible inhibitor.

Our ensuing analysis showed that active receptor synthesis and degradation also have implications in dose response. For instance, in Fig. 6, it is shown that when a slowly-dissociating irreversible drug is applied to a receptor under fast turnover, dose response may be highly similar to each other under a variety of incubation periods. Together with the previous example, it is inappropriate to conclude a drug is reversible given time-independent dose response either based on protein assay or *in vitro* cell assay.

The main purpose of this analysis is to demonstrate the relationship between dose response and parameter values. For the sake of simplicity, we only considered a linear model in which each reaction follows first-order kinetics. Results obtained in this paper are specific to the form of this linear model. In addition, we did not consider biological regulation over synthesis, degradation and sub-cellular localisation of a receptor [8]. In reality, receptor is often regulated under different levels, which often necessitates mechanistic modelling of a biological pathway to aid in interpretation of *in vitro* cell assays.

To further translate *in vitro* results into *in vivo* knowledge, Target Mediated Drug Disposition (TMDD) Models were developed to analyse receptor pharmacokinetics (PK) and pharmacodynamics (PD) in recent years. In addition to drug binding and receptor turnover, these models also consider the elimination of all species, to mimic *in vivo* conditions. They can be served as a useful theoretical framework. Model-based

analysis revealed that the necessary and sufficient condition for receptor rebound in a single dose animal experiment is that elimination rate of the drug-receptor product being slower than the elimination rates of the drug and of the receptor [9]. A time-scale analysis was also performed to provide accurate approximations of the temporal evolution under the assumption of high drug binding affinity [10]. These models share some parameters with the *in vitro* model described in this paper. For a drug discovery and development programme, the *in vitro* model should be used to identify parameter values from *in vitro* data. These parameters can be used subsequently to help identify the remaining parameter values in the *in vivo* model. This step-wise fitting may reduce uncertainty in parameter estimation. In this context, the *in vitro* model described in this paper improves the utility of TMDD models.

ACKNOWLEDGMENT

TY would gratefully acknowledge Hitesh Mistry (University of Manchester), James Yates (AstraZeneca UK Ltd) and Chris Brackley (University of Edinburgh) for useful discussions.

REFERENCES

- [1] P.K. Sorger, et al., "Quantitative and systems pharmacology in the post-genomic era: new approaches to discovering drugs and understanding therapeutic mechanisms," in An NIH white paper by the QSP workshop group, 2011, pp. 1-48.
- [2] P. Vicini, "Multiscale modeling in drug discovery and development: future opportunities and present challenges," Clin. Pharmacol. Ther., vol. 88, pp. 126-129, 2010.
- [3] D. Orrell, and E. Fernandez, "Using predictive mathematical models to optimise the scheduling of anti-cancer drugs," Innovations in Pharmaceutical Technology, vol. 33, pp. 58-62, 2010.
- [4] T.E. Yankeelov, et al., "Clinically relevant modeling of tumor growth and treatment response," Sci. Transl. Med., vol. 5, pp. 187ps189-187ps189, 2013.
- [5] P. Bonate, "What happened to the modeling and simulation revolution?," Clin. Pharmacol. Ther., vol. 96, pp. 416-417, 2014.
- [6] J. Strelow, et al., "Mechanism of Action assays for Enzymes," edited by J.I.M. Hughes et al., Assay Guidance Manual, 2012.
- [7] S. Nagar, J.P. Jones, and K. Korzekwa, "A Numerical Method for Analysis of In Vitro Time-Dependent Inhibition Data. Part 1. Theoretical Considerations," Drug Metab. Dispos., vol. 42, pp. 1575-1586, 2014.
- [8] D.A. Lauffenburger, and J.J. Linderman, Receptors: models for binding, trafficking, and signaling vol. 365: Oxford University Press New York., 1993.
- [9] P.J. Aston, G. Derks, B.M. Agoram, and P.H. van der Graaf, "A mathematical analysis of rebound in a target-mediated drug disposition model: I. Without feedback," J. Math. Biol., vol. 68, pp. 1453-1478, 2014.
- [10] L.A. Peletier, and J. Gabrielsson, "Dynamics of target-mediated drug disposition: characteristic profiles and parameter identification," J. Pharmacokinet. Phar., vol. 39, pp. 429-451, 2012.